We are IntechOpen,
the world's leading publisher of
Open Access books
Built by scientists, for scientists

6,900
Open access books available

186,000
International authors and editors

200M
Downloads

Our authors are among the

154
Countries delivered to

TOP 1%
most cited scientists

12.2%
Contributors from top 500 universities

CLARIVATE ANALYTICS

BOOK
CITATION
INDEX

INDEXED

WEB OF SCIENCE™

Selection of our books indexed in the Book Citation Index
in Web of Science™ Core Collection (BKCI)

Interested in publishing with us?
Contact book.department@intechopen.com

1

Tropical Channel Model

Pallav Ray[1], Chidong Zhang[2], Jim Dudhia[3],
Tim Li[1] and Mitchell W. Moncrieff[3]
[1]International Pacific Research Center (IPRC), University of Hawaii,
[2]Rosenstiel School of Marine and Atmospheric Science (RSMAS), University of Miami,
[3]National Center for Atmospheric Research (NCAR),
USA

1. Introduction

Numerical models are primary tools used for weather forecast and climate projections. Richardson (1922) made the first effort to predict weather numerically. Subsequently, a number of simple numerical and analytical models were proposed to explain the general circulation of the atmosphere (e.g., Charney, 1948; Eady, 1949; Philips, 1956; Matsuno, 1966; Gill, 1980). The present state-of-the-art models are constantly being evaluated and refined with the help of observations and theory to better understand the earth's weather and climate. Our gradual progress in developing and utilizing complex numerical models have lead to a hierarchy of models: i) atmospheric global climate models (AGCMs, Smagornisky et al., 1965; Benwell and Bretherton, 1968; Phillips and Shukla, 1973; Manabe, 1975; Simmons and Bengtsson, 1984); ii) coupled atmosphere-ocean GCMs (Manabe and Bryan, 1969); iii) hydrostatic and non-hydrostatic regional models (Wang and Halpern, 1970; Dudhia, 1993); (iv) cloud-system resolving models with regional domains (Grabowski et al. 1998; Grabowski and Moncrieff, 2001) and global domains (Miura et al., 2007; Satoh et al., 2008). A comprehensive review of the present day numerical models can be found in Tao and Moncrieff (2009).

Each category of model has advantages and disadvantages in terms of area coverage, spatial resolution, computational efficiency, and the representations of the physical processes; i.e., convection, microphysics, radiation, and surface exchange. Typically, regional models have higher resolution albeit a limited computational domain. On the other hand, GCMs with lower resolution cut the advantage of global coverage. A recent development is the introduction of tropical channel models (TCMs) which are defined as models that are global in the zonal direction but bounded in the meridional direction. A TCM has the following considerable advantages over the aforementioned modeling approaches: (1) A standard regional model needs boundary conditions in the zonal and the meridional directions, whereas a TCM is continuous in the east-west direction and thereby isolates the influences that arrive solely from the meridional boundaries (i.e., extratropics). It also allows free circumnavigation of tropical modes in the zonal direction. (2) The use of lateral boundary conditions only in the meridional direction enables a controlled quantification of the effects of extratropical disturbances on the tropics. 3) TCMs with nonhydrostatic dynamical cores

can have higher resolution and more sophisticated physics compared to GCMs. This is essential to capture the multi-scale organized convection in the tropics and its influence on the general circulation (Arakawa and Schubert, 1974; Chen et al., 1996; Houze, 2004; Moncrieff, 2010).

The objective of this chapter is to describe several TCMs that have been developed recently with an emphasis on their applications for the simulation and understanding of the tropical mean state and variabilty including the Madden-Julian oscillation (MJO), tropical cyclones (TCs) and double intertropical convergence zone (ITCZ).

Section 2 describes the models, data, and the design of the numerical simulations. Section 3 includes diagnoses of the simulations from three different TCMs. Section 4 summarizes the results along with the implications and limitations of the tropical channel model approach.

2. Model

We describe three different TCMs; two of them are constructed based on two different non-hydrostatic mesoscale models, and the third one is based on a hydrostatic GCM.

2.1 TCM based on MM5

A TCM was developed based on the fifth-generation Pennsylvania State University-National Center for Atmospheric Research (NCAR) Mesoscale Model (MM5; Dudhia, 1993; Grell et al., 1995). This atmosphere-only channel model employs a Mercator projection centered at the equator with open boundaries in the North-South direction. The model domain covers the entire tropics, with overlapping east-west boundaries. Tests ensured that simulated perturbations propagate zonally through the overlapping grids without distortion. Especially, two test runs are made in which the overlapping zone is located over the western Pacific and Atlantic Oceans, respectively. Results from these two simulations are the same over these regions with or without the overlapping zone. Hereafter, we refer to this tropical channel model as tropical MM5 (TMM5).

The dynamics and physics packages of TMM5 are same as those of the regular regional MM5, based on equations for a fully compressible, non-hydrostatic atmosphere. This TCM retains the two-way nesting capabilities. The spatial differencing is centered and of second order. There are 28 unevenly spaced full-sigma levels, with the maximum resolution in the boundary layer and the model top at 50 hPa. All nested domains are activated at the initial time of the simulation. The output is taken every 3 hours.

Several simulations are performed spanning between one to several weeks and are used to evaluate the skill of simulations by TMM5 against observations and reanalyses. Based on these tests and the work of Gustafson and Weare (2004a,b), the selected parameterizations are: (i) Betts-Miller convective scheme (Betts and Miller, 1986); (ii) explicit moisture calculations using a simple ice scheme (Dudhia, 1989); (iii) planetary boundary layer (PBL) scheme of the NCEP Eta model (Janjic, 1994), and (iv) Rapid Radiative Transfer Model longwave (RRTM, Mlïawer et al., 1997) and Dudhia (1989) shortwave radiation. The success of the Betts-Miller scheme, designed for the coarse resolution climate models, is perhaps because the simulations are in the hydrostatic regime at the resolutions employed (grid spacing of 111 and 37 km). Over the land, a 5-layer soil model option of the MM5 is used.

The model domains and the simulations are shown in Fig.1 and Table 1, respectively. The simulation 1DOM, with a model domain of 21°S-21°N, has a horizontal resolution of 111 km (D1 in Fig. 1). This is an ideal set up to study the intraseasonal varibility like the MJO which is of global scale in the zonal direction (Madden and Julian, 1971, 1972; Li and Zhou, 2009), and most of its variance is confined within the 20° latitude zones (Zhang and Dong, 2004). The purpose of the option of a two-way nested inner domain of 37 km over the Indian and western Pacific Oceans (D2 in Fig. 1) is to assess the effect of increasing horizontal resolution. This is our simulation 2DOM. Both simulations were integrated for four months from 1 March to 30 June, 2002, with sea surface temperature (SST) prescribed from observations (see section 2.4).
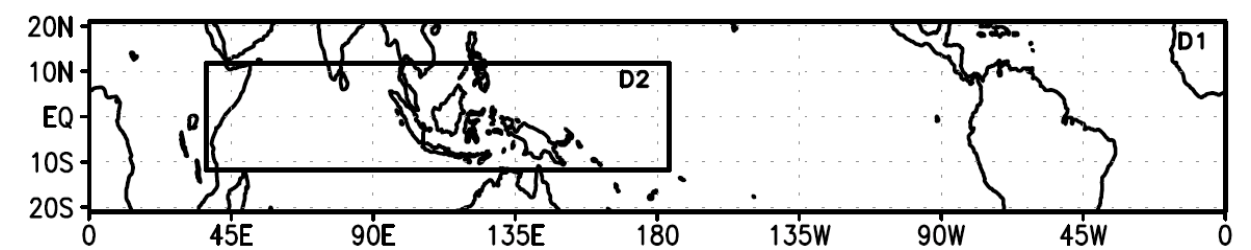

Fig. 1. Outer domain for the TMM5 (D1, 0-360°, 21°S-21°N) and the nested domain (D2, 37-183°E, 11°S-11°N). Domains D1 and D2 have resolutions of 111 km and 37 km, respectively.

Experiment	Integration Time	Remarks
1DOM	1 March- 30 June, 2002	Single domain simulation to test and validate the model
2DOM	1 March- 30 June, 2002	Nested domain (111 km / 37 km)

Table 1. The description of the simulations using the tropical channel MM5.

2.2 TCM based on WRF

Another tropical channel model is based on the Weather Research and Forecasting (WRF) model developed at the NCAR. We refer this as tropical WRF or TWRF (http://www.nrcm.ucar.edu). Conceptually, the configuration of TWRF is similar to TMM5. The horizontal grid-spacing of the TWRF is 36 km, and the meridional boundaries are placed at 30°S and 45°N. The model top is at 50 hPa, and 35 vertical levels are used. Output is archived every 3 hours. The configuration of the TWRF is shown in Fig. 2. The inner domains have grid-spacings of 12 km (domain D2 in Fig. 2) and 4 km (D3 in Fig. 2) respectively, and they are located over the warm pool region of the Indian and west Pacific oceans. Two-way interactions occur between the domains in the nested simulations. No cumulus parameterization is applied in the 4 km (cloud-system resolving) domain.

Preliminary simulations over the maritime continent evaluated the skill of the TWRF simulations. Based on these tests, the suite of parameterizations selected for this present study are: Kain-Fritsch cumulus parameterization (KF, Kain, 2004), WSM6 cloud microphysics (Hong et al., 2004), CAM 3.0 radiation scheme (Collins et al., 2006), YSU boundary layer

scheme (Hong et al., 2006), and Noah land surface model (Chen and Dudhia, 2001). Note that the Betts-Miller scheme (BM, Betts and Miller, 1986) available within the MM5 differs from the Betts-Miller scheme (BMJ, Janjic, 1994) available within the WRF.
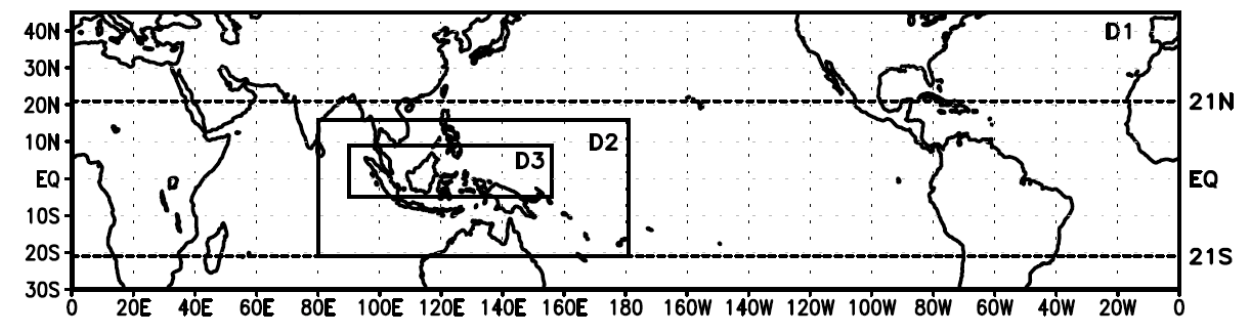

Fig. 2. Model domains for the tropical channel WRF (D1, 0°-360°, 30°S-45°N) and the nested domains (D2, 79°-183°E, 21°S-16°N and D3, 90°-157°E, 6°S-10°N). Domains D1, D2, and D3 have resolutions of 36 km, 12 km and 4 km, respectively. The simulation from 1996 to 2000 includes only the outer domain. The southern boundary was further moved to 45°S for the simulation from 1 December 1999 to 1 January 2006. The domain for the TMM5 is also marked here by the dashed lines (0°-360°, 21°S-21°N). See the text and Table 2 for further details.

The simulations using the TWRF are listed in Table 2. The simulation 1DOM in Table 2 is used to document the mean state. A similar multi-year simulation with a larger domain (1DOM_2 in Table 2) is also considered to evaluate its skill in capturing double ITCZ and tropical cyclones. Two other experiments (2DOM and 3DOM in Table 2) document the effect of increased horizontal resolution over the Indo-Pacific warm pool region.

Experiment	Integration Time	Description
1DOM	1 January 1996- 1 January 2001	1-way nested from NCEP-NCAR reanalysis with lateral boundaries at 30°S and 45°N
1DOM_2	1 December 1999-1 January 2006	Same as 1DOM, but with lateral boundaries at 45°S and 45°N
2DOM	1 January 1996-12 February 1998	2-way nested domains (36 km / 12 km)
3DOM	1 January 1997-1 July 1997	2-way nested domains (36 km / 12 km /4 km), 4 km domain is cloud resolving.

Table 2. The description of TWRF simulations. The horizontal resolution is 36 km for all the simulations except the nested runs (2DOM and 3DOM). See Fig. 2 for domain definitions and text for further details. [DOM : Domain].

2.3 TCM based on ECHAM4

TCMs based on regional models like MM5 and WRF, require boundary conditions from different datasets (other models or reanalysis). One disadvantage is that the variabilty in the prescribed boundary conditions may be different from the intrinsic variabilty produced by

the model. To overcome this problem, a GCM-based framework, in which the boundary conditions come from the parallel simulation ('control') of the same model can be used. Such a GCM-based framework also presents a global view of the atmospheric variabilty and can be used for forecasting.

The GCM used is the atmosphere-only ECHAM4, which captures the tropical variability reasonably well (Sperber et al., 2005; Lin et al., 2006; Zhang et al., 2006). The model is integrated for 20 years using the prescribed monthly SST. This is our control simulation ('control' in Table 3). In the other experiment ('NS' in Table 3), the model prognostic variables are nudged toward the 'controlled' annual cycle state over the 20°-30° latitudinal zone (red in Fig. 3) to remove the extratropical influences without interfering with the influences from the zonal direction. By comparing the simulations in the control and the NS experiments, the influences of the extratropics on the tropics can be estimated.
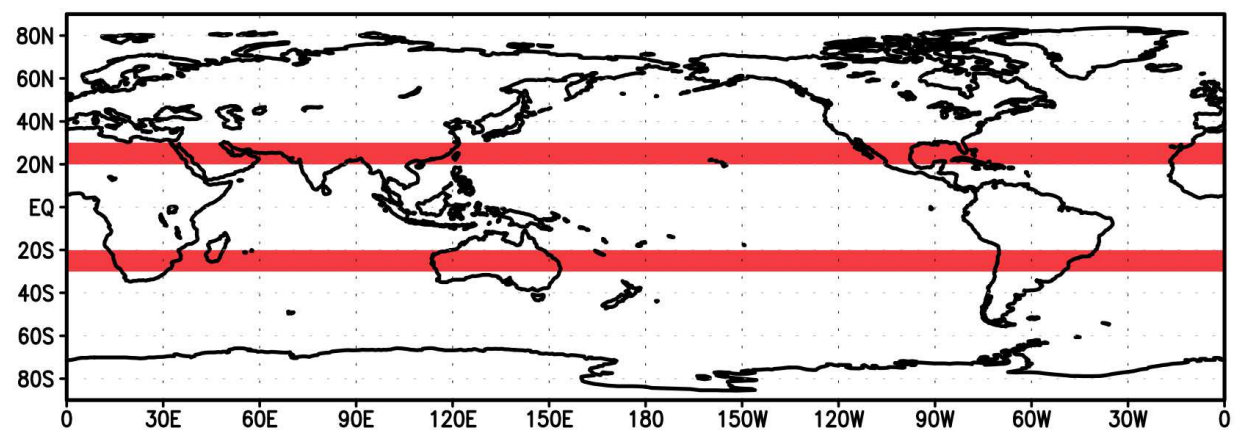

Fig. 3. Schematic diagram of the numerical experiments in which the prognostic variables in 20°-30° latitude zones (red) are relaxed toward the controlled climatological annual cycle. See text and Table 3 for further details.

Experiment	Description	Purpose
Control	ECHAM4 atmosphere only	To provide lateral boundary conditions for other simulations
NS	Relaxed to the annual cycle derived from the control simulation over 20°-30° latitudes	To evaluate the role of the extratropical influence on the tropics

Table 3. The description of the simulations using ECHAM4. (NS: North South).

2.4 Data

Model validation uses a number of observations and reanalyses data. They include: the NCEP-NCAR Re-analysis (Kalnay et al., 1996) winds; The European Centre for Medium-Range Weather Forecasts (ECMWF) 40-years Re-analysis (ERA40) winds (Uppala et al., 2005); Surface winds from the European Remote Sensing (ERS) satellites (Bentamy et al., 1999) and the NCEP-DOE Reanalysis (NCEP2, Kanamitsu et al., 2002); And two precipitation datasets including the merged analysis of precipitation (CMAP; Xie and Arkin, 1997), and the global precipitation climatological project (GPCP, Huffman et al., 1997) combined precipitation dataset.

The NCEP global tropospheric analyses (final or 'FNL' data, 1°x1°, 6 hourly) provide initial and lateral boundary conditions for the TMM5. The SSTs for TMM5 are also from this reanalysis, which contain intraseasonal fluctuations. The initial and boundary conditions of the TWRF are from the NCEP-NCAR reanalysis. The SSTs for TWRF are from the Atmospheric Model Intercomparison Project (AMIP; 1°x1°, 6-hourly; Taylor et al., 2000). For brevity, both reanalysis and CMAP/GPCP precipitation will be referred to as "observations".

3. Results

3.1 Tropical MM5 (TMM5)

The TMM5 simulations show considerable ability to capture an MJO event in comparison to most GCMs (Slingo et al., 1996; Lin et al., 2006; Zhang et al. 2006; Kim et al., 2009). The MJO event appeared in April-May 2002 (Fig. 4a), with the eastward propagating zonal wind anomalies switching from easterlies to westerlies on intraseasonal timescales. This event occured during a season in which the MJO is closest to the equator but, on average, is weaker than in other seasons (Zhang and Dong, 2004). After initiation, however, it propagated eastward at a speed slightly faster than the average phase speed of the MJO (5 m s^{-1}, marked by a straight line in Fig. 4a).

The start time (1 March) of the TMM5 simulations is about two months before the initiation of the MJO phase with active deep convection and low-level westerlies in May over the Indian Ocean. This choice of start time assesses the model's capability to reproduce the initiation of the MJO event, namely, the intraseasonal transition from low-level easterlies to westerlies (or from convectively inactive to active periods). In numerical models, forecast of future development of the MJO tends to have greater predictability when the MJO is already present at the initial time (Jones et al., 2000). Nevertheless, numerical experiments suggested predictability limit is about 10-15 days for rainfall, and about 25-30 days for upper-level winds (Waliser et al., 2003).

The results from the simulations 1DOM and 2DOM (Table 1) are shown in Fig. 4b and Fig. 4c, respectively. Simulated zonal winds at 850 hPa (hereafter U850) in D1 (middle panel) exhibits the same intraseasonal switch between easterly and westerly anomalies and eastward propagation over the Indian Ocean. Over the western Pacific, however, it moves faster than in reanalysis. This problem appears to be partially remedied by including the higher resolution nested domain D2 (Fig. 4c). In both simulations, the amplitudes of the anomalies are larger than that in reanalysis. Notice that the westward propagating synoptic-scale westerly anomalies embedded in the MJO envelope over the Indian Ocean are captured by the simulation with the nested domain (2DOM in Table 1). These detailed structures in simulated anomalies are perhaps due to the higher resolution of the model.

The most interesting result from this simulation is that the initiation of the MJO event over the Indian Ocean is reproduced by the model at about the same time as shown by reanalysis two months after the model initial time. The MJO is thought to be unpredictable beyond two to three weeks (e.g., Waliser et al., 2003). If this is correct, then the reproduction of the U850 anomalies by TMM5 cannot be attributed to the initial conditions.

The above results lead to a hypothesis that this MJO event is generated by the influences from the lateral boundaries. This hypothesis is supported by a series of sensitivity tests that

demonstrate that the simulated MJO initiation is critically dependent on the time-varying lateral boundary conditions from the reanalysis (Ray et al., 2009). When such lateral boundary conditions are replaced by time-independent conditions, the model fails to reproduce the MJO initiation. In particular, the diagnoses of the zonal momentum budget for the MJO initiation region reveals that the advection by meridional winds is important prior to the initiation of this MJO (Ray and Zhang, 2010).
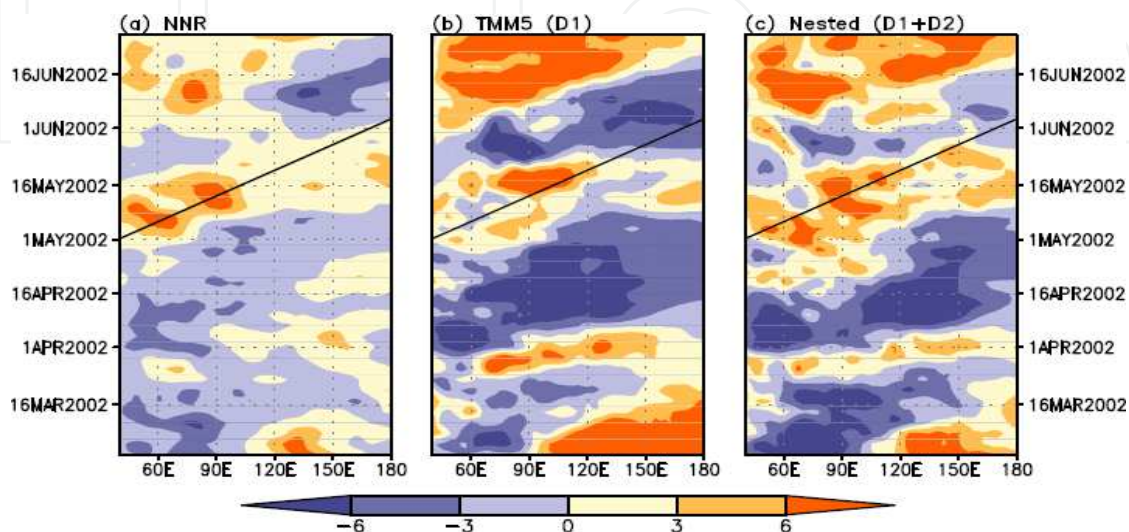

Fig. 4. Time-longitude diagrams of daily U850 anomalies (m s^{-1}) averaged over 10°S-10°N from the (a) NCEP-NCAR reanalysis (NNR), (b) TMM5 single domain simulation (1DOM in Table 1), and (c) TMM5 nested domain simulation (2DOM in Table 1). A 3-day running mean is applied.

3.2 Tropical WRF (TWRF)

We describe the performance of the TWRF in terms of its ability to capture the mean precipitation, double ITCZ, and hurricane statistics.

3.2.1 Mean state

Fig. 5 shows the mean precipitation from two different datasets and TWRF simulation (1DOM in Table 2). The model lacks precipitation over the equatorial Indian Ocean and the west African monsoonal region. However the model overestimates precipitation in the west Pacific, particularly in the region north of maritime continent and in the south Pacific convergence zone (SPCZ). The error in the mean state is found to be a primary reason for the poor simulation of the MJO in this model (Ray et al., 2011), even when higher resolution nested domains are included (2DOM and 3DOM in Table 2). However, such error does not seem to affect the simulation of convectively coupled Kelvin waves in the model (Tulich et al., 2011). Overall, precipitation is overestimated in the southern hemishere, and underestimated close to the equator (5°S-5°N, Murthi et al., 2011). The large bias in the precipitation over the southern Indian Ocean was thought to be due to the interactions between tropical cyclones and the southern boundaries. To rectify this problem, southern boundaries are further moved to 45°S in another experiment (1DOM_2 in Table 2). However, this does not improve the result significantly, indicating potential

problems with the model physics (Tulich et al., 2011; Murthi et al., 2011). Nevertheless, the model reasonably captures the initiation of certain MJO events that are influenced by the extratropics (Ray et al., 2011), and genesis of tropical cyclones from easterly waves (see section 3.2.3).
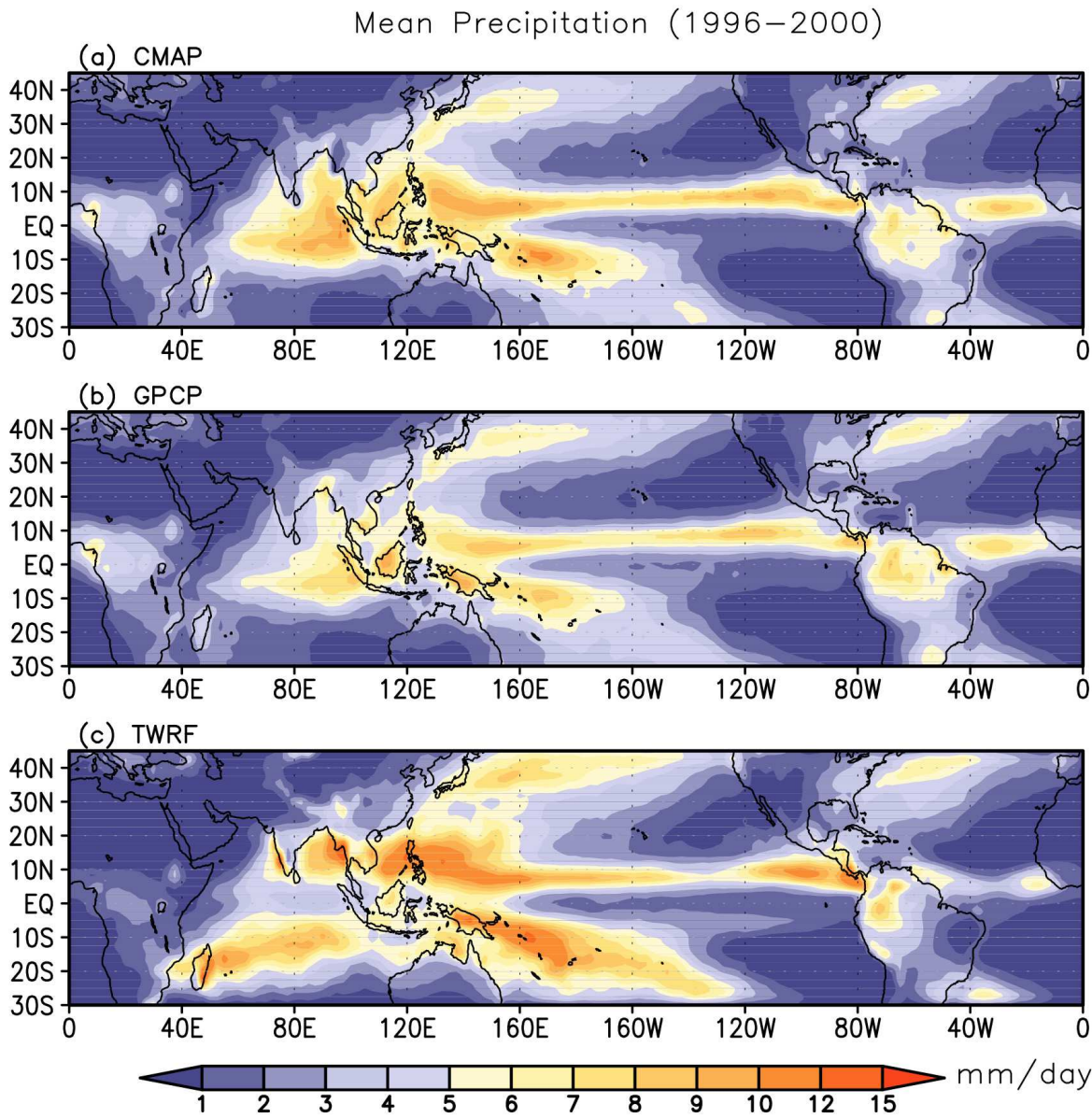

Fig. 5. Annual mean rainfall (mm day^{-1}) during 1996-2000 from the (a) CMAP (b) GPCP and (c) TWRF simulation 1DOM in Table 2.

3.2.2 Double ITCZ

It is known that the presence of a too-strong double ITCZ in the Pacific is a common bias in AGCMs (e.g., Meehl and Arblaster, 1998), as well as in the coupled GCMs (Mechoso et al., 1995). We examine the double ITCZ with respect to surface wind convergence and precipitation over the eastern Pacific, since the double ITCZ is most prominent over the eastern Pacific during March and April (Zhang, 2001).

Figure 6 shows the seasonal cycles in SST (shaded) and surface wind divergence (contoured) over the equatorial eastern Pacific (100°W-140°W). Note that our simulation period includes the strong ENSO event of 1997-98 (McPhaden, 1999). During March-April, the convergence south and north of the equator is captured well by the model. Over the equator, the observations show weak convergence, but the simulation indicates divergence. During boreal summer, the model shows much stronger convergence south of the equator compared to the observations. Overall, the TWRF has a distinct double ITCZ and no significant improvement occurred when nested domains were employed.
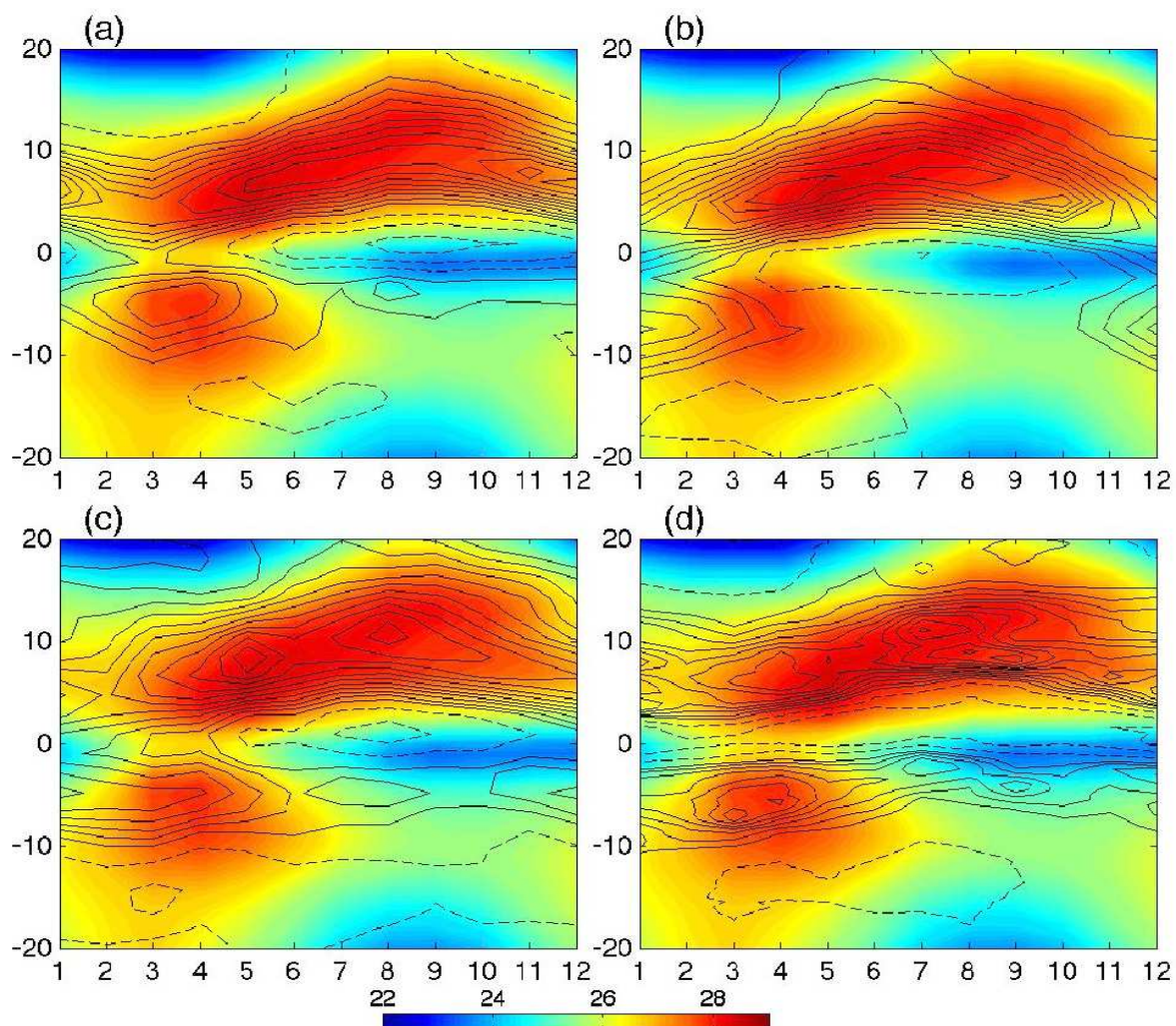
Fig. 6. Seasonal cycles of SST (shaded, °C) and surface wind divergence (contours, 10^6 s^{-1}) from the (a) ERS, (b) ERA40, (c) NCEP2, and (d) TWRF. All are averaged over the eastern Pacific (100°W-140°W) during the period 1996-2000. Solid (dashed) contours represent convergence (divergence).

3.2.3 Tropical cyclones

Using an objective tracking algoritm similar to Walsh et al. (2004), Tulich et al. (2011) estimated the genesis locations and tracks of tropical cyclones from the model simulation 1DOM_2 (Table 2). Fig. 7 shows the latitudinal distribution of TC genesis events over three

different ocean basins. The error in the distribution is presumably due to the error in the model's easterly wave climatology that is intimately linked to the genesis of TCs (Landsea, 1993; Frank and Roundy, 2006). The model greatly overestimates the number of storms over the western Pacific (Fig. 7a), but underestimates over the north Atlantic (Fig. 7c). The model also overestimates over the eastern Pacific (Fig. 7b). Overall, while the TWRF simulation captures the global and seasonal distribution of tropical cyclones, their numbers are overestimated.

However, the simulation with a nested domain of 12 km over the Atlantic during the 2005 hurricane season produces resonable cyclone statistics (Fig. 8, Done et al., 2011). Compared to 27 observed tropical storms, the model produces 29 storms, indicating great improvement with the increase in the horizontal resolution.
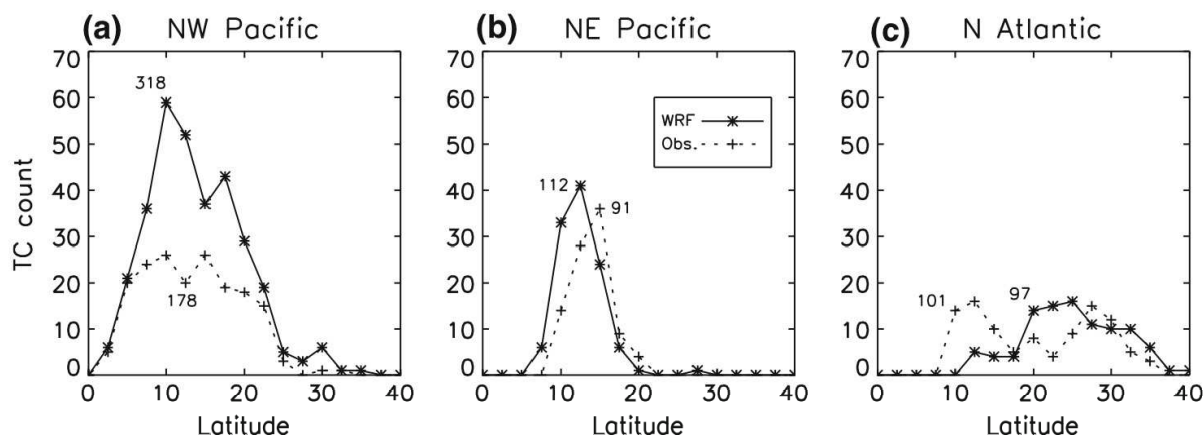
Fig. 7. Histogram of TC genesis events versus latitude for the TWRF (sold) and observations (dashed) over the (a) NW Pacific, (b) NE Pacific, and (c) N Atlantic. The total number of genesis events are indicated next to the corresponding histogram. (From Tulich et al., 2011).
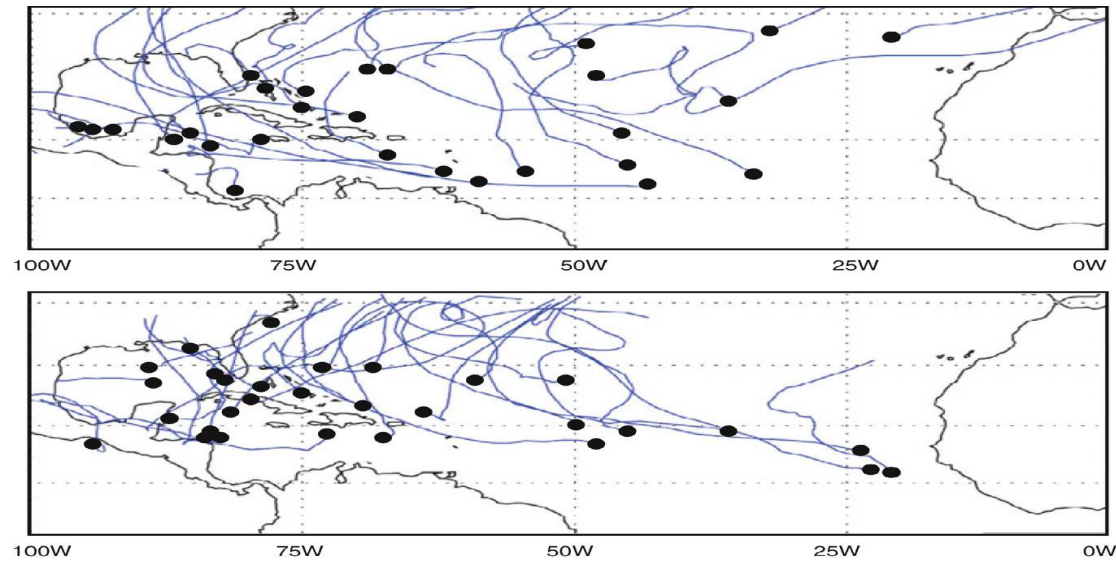

Fig. 8. Initial locations (black circles) and tracks (blue lines) of tropical cyclones in the Atlantic Basin during 2005 in (top) the IBTrACS dataset and (bottom) TWRF simulation. (From Done et al., 2011).

3.3 Tropical ECHAM4

Fig. 9 compares the simulated mean state from the observations and the model over the Indo-Pacific region. Lower tropospheric winds are westerly over the Indian Ocean (Fig. 9a, shaded) but easterlies prevail in the upper troposphere (Fig. 9a, contoured). This is captured well by the control simulation (Fig. 9b). However, in the experiment NS (Table 3), U850 is weaker over the equatorial western Indian Ocean, and U200 is of opposite sign over much of the Indian Ocean (Fig. 9c), and is underestimated over the west Pacific. The precipitation and OLR in the control (Fig. 9e) are similar to those in the observations (Fig. 9d), although precipitation (OLR) is everestimated (underestimated). Note that unlike TWRF, the control simulation does not lack precipitation over the equatorial Indian Ocean (Fig. 5c). However, in the NS, precipitation is significantly reduced over the equatorial Indian Ocean, and is increased over the SPCZ region (Fig. 9f). The ITCZ is shifted further from the equator in NS, with very little precipitation north of the equatorial Pacific. The MJO variance in the NS is also reduced substantially compared to the control indicating possible influences from the extratropics. To what extent the mean state is responsible for the lack of variability remains to be investigated more thoroughly (Ray and Li, 2011).
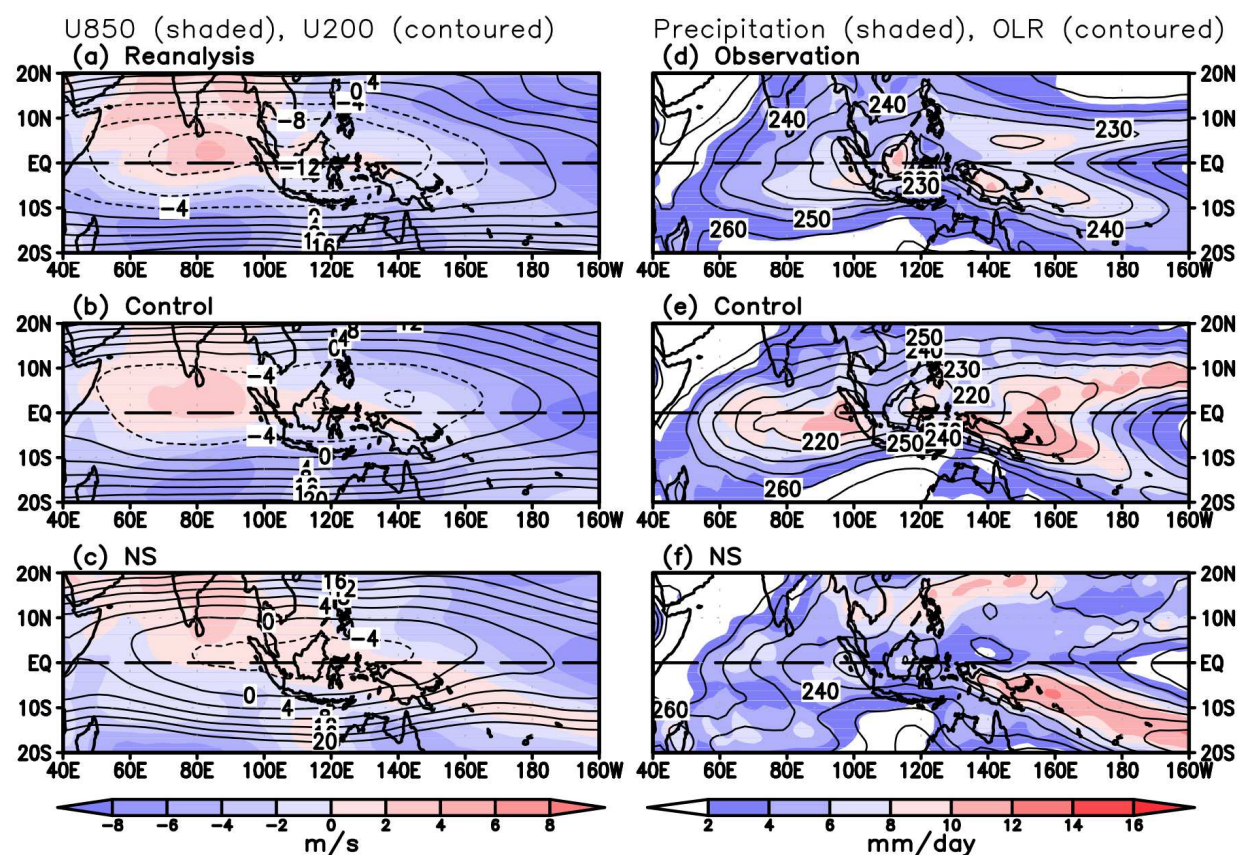

Fig. 9. (left) Mean zonal winds at 850 hPa (U850, m s^{-1}, shaded) and at 200 hPa (U200, m s^{-1}, contoured). (right) Mean precipitation (mm day^{-1}, shaded) and OLR (W m^{-2}, contoured). All are averaged over 20 years. Contour intervals are 4 m s^{-1} for U200, and 10 W m^{-2} for OLR. For U200, solid (dashed) lines represent westerlies (easterlies).

4. Conclusion

Tropical channel models (TCMs) are defined as models that are global in the zonal direction but bounded in the meridional direction. Such a model can be constructed using existing regional models or even the GCMs. Two TCMs based on regional models MM5 and WRF, and the third one based on the ECHAM4 GCM, were described. Although all three TCMs are atmosphere only, they could be coupled to an ocean model. Therefore the TCM is a unique tool to study the tropics and its interactions with the extratropics.

The simulations using TCMs are far from perfect. There are biases in the mean state, ITCZ, MJO, and other tropical modes. The gross fetures of an MJO event are reproduced after two months from the start of simulation using the TCM based on MM5 (TMM5). This is well beyond the usual MJO predictability limit of 15-20 days associated with global models (Waliser et al., 2003). The TCM simulations are forced by prescribed boundary conditions, and are not initial value problems. Longer integration of another TCM based on WRF (TWRF) does not lead to better tropical variabilty compared to that in GCMs. This is unexpected since, compared to a GCM, a TCM simulation has the added constraint of specified meridional boundary conditions. The error in the mean state is a possible reason for the poor representation of tropical variabilty in TWRF. It is not known to what extent the error in the mean state inhibits tropical variabilty, although it is likely to be model dependent.

These studies suggest a new practice in tropical prediction: a high-resolution domain of the tropics nested within a relatively coarse-resolution global model. The latter is known to suffer less from deficiencies in cumulus parameterizations in the extratropics because of the strong dynamic large-scale control of convection there. This approach of global nested domains, currently being explored by some modeling groups, permits two-way tropical-extratropical interactions with a more precise treatment of tropical convection and much more computational efficiency than a global high-resolution model. The results call for further attention to the untapped potential of high-resolution nonhydrostatic models (Moncrieff et al., 2007) in the simulation and forecasting of tropical atmospheric convection, such as that undertaken within the WCRP-WWRP/THORPEX coordinated project, the Year of Tropical Convection (YOTC, Waliser and Moncrieff, 2008; see www.ucar.edu/yotc).

## 5. Acknowledgment

6. References

Arakawa, A., & Schubert, W.H. (1974). Interaction of a cumulus cloud ensemble with the large-scale circulation. Part I, *J. Atmos. Sci.*, Vol.31, pp. 674-701

Bentamy, A.; Queffeulou, Y.; Quilfen, Y. & Katasaros, K. (1999). Ocean surface wind fields estimated from satellite active and passive microwave instruments. *IEEE Trans. Geosci. Sensing*, Vol.37, pp. 2469-2486

Benwell, G., & Bretherton, F. (1968). A pressure oscillation in a ten-level atmospheric model. *Quart. J. Roy. Meteor. Soc.*, Vol.94, pp. 123-131

Betts, A.K. & Miller, M.J. (1986). A new convective adjustment scheme. II. Single column testing using GATE wave, BOMEX, ATEX, and arctic air-mass data sets. *Quart. J. Roy. Meteor. Soc.*, Vol.112, pp. 693-709

Charney, J.G. (1948). On the scale of atmospheric motions. *Geophys. Publ.*, Vol.17, No.2, pp. 1-17

Chen, F. & Dudhia, J. (2001). Coupling an advanced land surface-hydrology model with the Penn State-NCAR MM5 modeling system, Part I: Model implementation and sensitivity. *Mon. Wea. Rev.*, Vol.129, pp. 569-585

Chen, S.S.; Houze, R.A. & Mapes, B.E. (1996). Mult-scale variabilty of deep convection in relation to large-scale circulation in TOGA-COARE. *J. Atmos. Sci.*, Vol.53, pp. 1380-1409

Collins, W.D.;Bitz, C.M.; Blackmon, M.L.; Bonan, G.B.; Bretherton, C.S.; Carton, J.A.; Chang, P.; Doney, S.C.; Hack, J.J.; Henderson, T.B.; Kiehl, J.T.; Large, W.G.; McKenna, D.S.; Santer, B.D. & Smith, R.D. (2006). The Community Climate System Model: CCSM3. *J. Clim.*, Vol.19, pp. 2122-2143

Done, J.M.; Holland, G.J. & Webster, P.J. (2011). The role of wave energy accumulation in tropical cyclogenesis over the tropical north Atlantic. *Clim. Dyn.*, Vol.36, pp. 753-767, doi 10.1007/s00382-010-0880-5

Dudhia, J. (1989). Numerical study of convection observed during the Winter Monsoon Experiment using a mesoscale two-dimensional model. *J. Atmos. Sci.*, Vol.46, pp. 3077-3107

Dudhia, J. (1993). A nonhydrostatic version of the Penn State-NCAR Mesoscale Model: Validation tests and simulation of an Atlantic cyclone and cold front. *Mon. Wea. Rev.*, Vol.121, pp. 1493-1513

Eady, E.T. (1949). Long waves and cyclone waves. *Tellus*, Vol.1, No.3, pp. 33-52

Frank, W.M. & Roundy, P.E. (2006). The role of tropical waves in tropical cyclogenesis. *Mon. Wea. Rev.*, Vol.134, pp. 2397-2417

Gill, A. (1980). Some simple solutions for heat-induced tropical circulation. *Quart. J. Roy. Meteor. Soc.*, Vol.106, pp. 447-462

Grabowski, W.W.; Wu, X., Moncrieff, M.W. & Hall, W.D. (1998). Cloud-resolving modeling of cloud systems during Phase III of GATE. Part II: Effects of resolution and the third spatial dimension. *J. Atmos. Sci.*, Vol.55, pp. 3264-3282

Grabowski, W.W. & Moncrieff, M.W. (2001). Large-scale organization of tropical convection in two-dimensional explicit numerical simulations. *Quart. J. Roy. Meteor. Soc.* Vol.127, pp. 445-468

Grell, G.A.; Dudhia, J. & Stauffer, D.R. (1995). A description of the fifth-generation Penn-State/NCAR Mesoscale Model (MM5). NCAR/TN-398.

Gustafson, W.I. & Weare, B.C. (2004a). MM5 modeling of the Madden-Julian oscillation in the Indian and west Pacific Oceans: Model description and control run results. *J. Clim.*, Vol.17, pp. 1320-1337

Gustafson, W.I. & Weare, B.C. (2004b). MM5 modeling of the Madden-Julian oscillation in the Indian and west Pacific Oceans: Implications of 30-70 day boundary effects on MJO development. *J. Clim.*, Vol.17, pp. 338-1351

Hong, S.-Y.; Dudhia, J. & Chen, S.-H. (2004). A revised approach to ice microphysical processes for the bulk parameterization of clouds and precipitation. *Mon. Wea. Rev.*, Vol.132, pp. 103-120

Hong, S.-Y.; Noh, Y. & Dudhia, J. (2006). A new diffusion package with an explicit treatment of entrainment processes. *Mon. Wea. Rev.*, Vol.134, pp. 2318-2341

Houze, R.A. (2004). Mesoscale convective systems. *Rev. Geophys.*, Vol.42, RG4003, doi:10.1029/2004RG000150

Huffman, G.J. & Coauthors (1997). The global precipitation climatology project (GPCP) combined precipitation dataset. *Bull. Amer. Meteor. Soc.*, Vol.78, pp. 5-20

Janjic, Z.I. (1994). The step-mountain coordinate model: Further development of the convection, viscous sublayer, and turbulence closure schemes. *Mon. Wea. Rev.*, Vol.122, pp. 927-945

Jones, C.; Waliser, D.E.; Schemm, J.K.E. & Lau, W.K.M. (2000). Prediction skill of the Madden-Julian oscillation in dynamical extended range forecasts. *Clim. Dyn.*, Vol.16, pp. 273-289

Kain, J.S. (2004). The Kain-Fritsch convective parameterization: An update. *J. Appl. Meteorol.*, Vol.43, pp. 170-181

Kalnay, E. & Coauthors (1996). The NCEP-NCAR 40-year reanalysis project. *Bull. Amer. Meteor. Soc.*, Vol.77, pp. 437-471

Landsea, C.W. (1993). A climatology of intense (or major) Atlantic hurricanes. *Mon. Wea. Rev.*, Vol.121, pp. 1703-1713

Kanamitsu, M.; Ebisuzaki, W.; Woollen, J.; Yang, S.-K.; Hnilo, J.J.; Fiorino, M. & Potter, G.L. (2002). NCEP-DOE AMIP-II Reanalysis (R-2). *Bull. Amer. Meteor. Soc.*, Vol.83, pp. 1631-1643.

Kim, D. & Coauthors (2009). Application of MJO simulation diagnostics to climate models. *J. Clim.*, Vol.22, 6413-6436

Li, T. & Zhou, C. (2009). Planetary scale selection of the Madden-Julian oscillation. *J. Atmos. Sci.*, Vol.66, pp. 2429-2443

Lin, J.-L., & Coauthors (2006). Tropical intraseasonal variability in 14 IPCC AR4 climate models. Part I: Convective signals. *J. Clim.*, Vol.19, 2665-2690

Madden, R.A. & Julian, P.R. (1971). Detection of a 40-50 day oscillation in the zonal wind in the tropical Pacific. *J. Atmos. Sci.*, Vol.28, pp. 702-708

Madden, R.A. & Julian, P.R. (1972). Description of global-scale circulation cells in the tropics with a 40-50 day period. *J. Atmos. Sci.*, Vol.29, pp. 1109-1123

Manabe, S., & Bryan, K. (1969). Climate calculations with a combined ocean-atmosphere model. *J. Atmos. Sci.*, Vol.26, No.4, pp. 786-789

Manabe, S. (1975). The use of comprehensive general circulation modeling for studies of the climate and climate variation, the physical basis of climate and climate modeling. Report of the International Study Conference in Stockholm, *GARP Publication Series*, Vol.16, pp. 148-162

Matsuno, T. (1966). Quasi-geostrophic motions in the equatorial area. *J. Meteorol. Soc. Jpn.*, Vol.44, pp. 25-43

McPhaden, M.J. (1999). Genesis and evolution of the 1997-98 El Nino. *Science*, Vol.283, pp. 950-954

Mechoso, C.R. & Coauthors (1995). The seasonal cycle over the tropical Pacific in coupled ocean-atmosphere general circulation models. *Mon. Wea. Rev.*, Vol.123, pp. 2825-2838

Meehl, G.A. & Arblaster, J.M. (1998). The Asian-Australian monsoon and El Niño Southern Oscillation in the NCAR Climate System Model. *J. Clim.*, Vol.11, pp. 1356-1385

Miura, H.; Satoh, M.; Nasuno, T., Noda, A.T. & Oouchi, K. (2007). A Madden-Julian oscillation event realistically simulated by a global cloud-resolving model. *Science*, Vol.318, pp. 1763-1765

Mlawer, E.J.; Taubman, S.J.; Brown, P.D.; Jacono, M.J. & Clough, S.A. (1997). Radiative transfer for inhomogeneous atmosphere: RRTM, a validated correlated-k model for the longwave. *J. Geophys. Res.*, Vol.102, pp. 16663-16682

Moncrieff, M.W. (2010). The multi-scale organization of moist convection and the interaction of weather and climate, In D.-Z. Sun and F. Bryan (Eds.), Climate Dynamics: Why Does Climate Vary? *Geophysical monograph series*, Vol.189, American Geophysical Union, Washington DC, 3-26, doi:10.1029/2008GM000838

Moncrieff, M.W.; Shapiro, M.A.; Slingo, J.M. & Molteni, F. (2007). Collaborative research at the intersection of weather and climate. *WMO Bulletin*, Vol. 56, pp. 1-9

Murthi, A.; Bowmann, K.P. & Leung, L.R. (2011). Simulations of precipitation using NRCM and comparisons with satellite observations and CAM: annual cycle. *Clim. Dyn.* (in press)

Phillips, N.A. (1956). The general circulation of the atmosphere: A numerical experiment. *Quart. J. Roy. Meteorol. Soc.*, Vol.82, pp. 123-164

Phillips, N.A. & Shukla, J. (1973). On the strategy of combining coarse and fine grid meshes in the numerical weather predition models. *J. Appl. Meteorol.*, Vol.12, pp. 736-770

Ray, P.; Zhang, C.; Dudhia, J. & Chen S.S. (2009). A numerical case study on the initiation of the Madden-Julian oscillation. *J. Atmos. Sci.*, Vol.66, pp. 310-331

Ray, P. & Zhang, C. (2010). A case study of the mechanics of extratropical influence on the initiation of the Madden-Julian oscillation. *J. Atmos. Sci.*, Vol.67, pp. 515-528

Ray, P.; Zhang, C.; Moncrieff, M.W.; Dudhia, J., Caron, J., Leung, L.R. & Bruyere, C. (2011). Role of the atmospheric mean state on the initiation of the Madden-Julian oscillation in a tropical channel model. *Clim. Dyn.*, Vol.36, pp. 161-184, doi 10.1007/s00382-010-0859-2

Ray, P. & Li, T. (2011). On the relative roles of the circumnavigating waves and the extratropics on the Madden-Julian oscillation (MJO), (in preparation).

Richardson, L.F. (1922). Weather prediction by numerical process. Cambridge University press (reprt. Dover).

Satoh, M.; Matsuno, T.; Tomita, H.; Miura, H.; Nasuno, T. & Iga, S. (2008). Nonhydrostatic icosahedral atmospheric model (NICAM) for global cloud resolving simulations. *J. Comp. Phys.*, Vol.227, pp. 3486-3514

Simmons, A.J., & Bengtsson, L. (1984). Atmospheric general circulation models: Their design and use for climate studies. In The Global Climate, ed. J. T. Hougton. Cambridge University Press., Cambridge, pp. 37-62

Slingo J.M., and Coauthors (1996) Intraseasonal oscillations in 15 atmospheric general circulation models: Results from an AMIP diagnostic subproject. *Clim. Dyn.*, Vol.12, pp. 325-357

Smagorinsky, J.; Manabe, S. & Holloway, Jr. J.L. (1965). Numerical results from a nine-level general circulation model of the atmosphere. *Mon. Wea. Rev.*, Vol.93, No.12, pp. 727-768

Sperber, K.P.; Gualdi, S.; Legutke, S. & Gayler, V. (2005). The Madden–Julian oscillation in ECHAM4 coupled and uncoupled general circulation models. *Clim. Dyn.*, Vol.25, pp. 117–140

Tao, W.-K. & Moncrieff, M.W. (2009). Multiscale cloud system modeling. *Rev. Geophys.*, Vol.47, RG40002, doi:10.1029/2008RG000276

Taylor, K.E.; Williamson, D. & Zwiers, F. (2000). The sea surface temperature and sea-ice concentration boundary conditions for AMIP II simulations. PCMDI Report No. 60 and UCRL-MI-125597, 25 pp

Tulich, S.N.; Kiladis, G.N. & Suzuki-Parker, A. (2011). Convectively coupled Kelvin and easterly waves in a regional climate simulation of the tropics. *Clim. Dyn.*, Vol.36, pp. 185-203, doi 10.1007/s00382-009-0697-2

Uppala, S.M. & Coauthors (2005). The ERA-40 reanalysis. *Quart. J. Roy. Meteorol. Soc.*, Vol.131, pp. 2961-3012

Waliser, D.E.; Lau, K.M.; Stern, W. & Jones, C. (2003). Potential predictability of the Madden-Julian oscillation. *Bull. Amer. Meteor. Soc.*, Vol.84, pp. 33-50

Waliser, D.E. & Moncrieff, M.W. (2008). Year of Tropical Convection (YOTC) Science Plan, WMO/TD-No. 1452, WCRP -130, WWRP/THORPEX, No.9, 26 pp

Wang, H.-H., & Halpern, P. (1970). Experiments with a regional fine-mesh prediction model. *J. Appl. Meteor.*, Vol.9, pp. 545-553

Walsh, K.J.E.; Nguyen, K.-C. and McGregor, J.L. (2004). Fine resolution regional climate model simulations of the impact of climate change on tropical cyclons near Australia. *Clim. Dyn.*, Vol.22, pp. 47-56

Xie, P. & Arkin, P.A. (1997). Global precipitation: A 17-year monthly analysis based on gauge observations, satellite estimates, and numerical model outputs. *Bull. Amer. Meteor. Soc.*, Vol.78, pp. 2539-2558

Zhang, C. (2001). Double ITCZs. *J. Geophys. Res.*, Vol.106, No.D11, pp. 11785-11792

Zhang, C. & Dong, M. (2004). Seasonality of the Madden-Julian oscillation. J. *Clim.*, Vol.17, pp. 3169-3180

Zhang, C. (2005). Madden-Julian oscillation. *Rev. Geophys.*, Vol.43, RG2003, doi:10.1029/2004RG000158

Zhang, C.; Dong, M.; Gualdi, S.; Hendon, H.H.; Maloney, E.D.; Marshall, A.; Sperber, K.R. & Wang, W. (2006). Simulations of the Madden-Julian oscillation by four pairs of coupled and uncoupled global models. *Clim. Dyn.*, DOI: 10.1007/s00382-006-0148-2
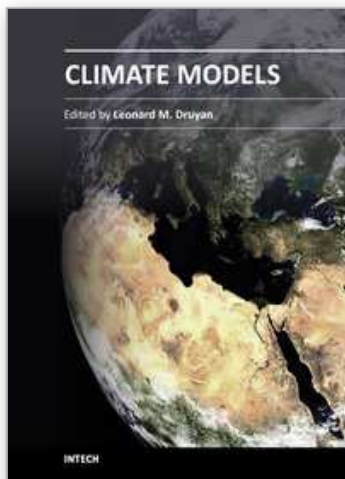
Climate Models

Edited by Dr. Leonard Druyan

Climate Models offers a sampling of cutting edge research contributed by an international roster of scientists. The studies strive to improve our understanding of the physical environment for life on this planet. Each of the 14 essays presents a description of recent advances in methodologies for computer-based simulation of environmental variability. Subjects range from planetary-scale phenomena to regional ecology, from impacts of air pollution to the factors influencing floods and heat waves. The discerning reader will be rewarded with new insights concerning modern techniques for the investigation of the natural world.

How to reference

In order to correctly reference this scholarly work, feel free to copy and paste the following:

INTECH

open science | open minds